CLUSTERING IN ^{11,12,13}C*

L. Palada[a], N. Soić[a], L. Acosta[b], S. Bailey[c], D. Dell'Aquila[a]
J.A. Duenas[b], J.P. Fernandez Garcia[d], P. Figuera[d]
E. Fioretto[e], M. Fisichella[d], L. Grassi[a], O. Kirsebom[f]
T. Kokalova Wheldon[c], M. Lattuada[d], G. Marquinez Duran[b]
I. Martel[b], T. Mijatović[a], L. Prepolec[a], N. Skukan[a], R. Smith[c]
S. Szilner[a], V. Tokić[a], M. Uroić[a], N. Vukman[a], J. Walshe[c]
C. Wheldon[c]

[a]Ruđer Bošković Institute, Zagreb, Croatia
[b]University of Huelva, Huelva, Spain
[c]University of Birmingham, Birmingham, United Kingdom
[d]INFN Laboratori Nazionali del Sud, Catania, Italy
[e]INFN Laboratori Nazionali di Legnaro, Legnaro, Italy
[f]University of Aarhus, Aarhus, Denmark

Received 28 November 2023, accepted 23 January 2024, published online 24 April 2024

Characterization of the excited states of ^{11}C, ^{12}C, ^{13}C isotopes was performed using experimental data collected at the INFN-LNL in Italy. The study employed a 95 MeV ^{14}N beam on ^{10}B targets to probe clustering phenomena in carbon isotopes. The experimental setup included a detector system covering polar angles from 15° to 72°, enabling the study of reactions with two and three products in the exit channel. Analysis of the three-product exit channels is presented to provide insight into the process of analyzing such reactions. Presented results for the ^{7}Be + ^{4}He, ^{8}Be + ^{4}He, and ^{9}Be + ^{4}He decays of ^{11}C, ^{12}C, ^{13}C, respectively, unveil states at 7.6, 9.7, and 14.1 MeV in ^{12}C, 8.1 and 8.4 MeV in ^{11}C, as well as a broad peak centered at 13.6 MeV with a possible contribution of states from 13.4 to 14.1 MeV in ^{13}C. The detection of these states serves as a crucial validation of the analysis and data selection procedures, representing an initial step before exploring other exit channels.

DOI:10.5506/APhysPolBSupp.17.3-A31

1. Introduction

Light nuclei are an excellent laboratory to examine the basic principles of nuclear structure and interaction. Both aspects of nuclear structure,

* Presented at the XXXVII Mazurian Lakes Conference on Physics, Piaski, Poland, 3–9 September, 2023.

single-particle dynamics and nucleon correlations which result in clustering, are most pronounced in light nuclei due to a small number of degrees of freedom in these systems. Understanding the correlations and formation of clusters is closely related to fine details of the nuclear force as well as to spatial and quantum symmetries within the nuclei. Modern nuclear theories such as Antisymetrized Molecular Dynamics, Continuum Monte Carlo Method, No Core Shell Model, and models using Effective Field Theory on the lattice [1], are able to realistically model $A < 20$ nuclei starting from individual nucleons and the first principles, making possible detailed comparisons of calculated nuclear properties with phenomenological approaches and high-precision experimental data. To benchmark these newly developed models, is of prime importance to obtain experimental data for a large set of light nuclei over a large range of N/Z ratios.

The structure of the lightest-element nuclei can be understood in a picture based on α particle as the main building unit, for example, see review papers [2, 3]. It emerged that one of the key nuclei to understand α clustering is ^{12}C whose low excitation level scheme corresponds to that for an assembly of three α particles. The $^{8}\mathrm{Be} + \alpha$ cluster structure of the first unbound 0^+ state, the Hoyle state, strongly enhances the 3α fusion process, a key reaction for energy production in the second step of the star evolution and for the nucleosynthesis of carbon, the seed for production of all heavier elements. Studies have revealed the existence of the 2^+ rotational excitation of the Hoyle state [4–6], while for the possible 4^+ member of the band, some indications are found [7]. Also, more states have been recently found at higher excitation energies [8–10] and their 3α cluster configuration has yet to be confirmed.

Numerous studies have shown that quite exotic structural phenomena appear away from the $N \approx Z$ stability line, one of them being the occurrence of nuclear molecules. A nuclear molecule is a system built from α clusters and valence neutrons in the orbitals which can be constructed as the linear combinations of the orbitals around the individual α particles. The covalent exchange of the neutrons between the α cores increases the stability of the system, very similar to the binding of covalent atomic molecules. The two-center nuclear molecular structure has been identified so far in beryllium isotopes, particularly in ^{10}Be [11–13] and ^{12}Be [14]. Indications for more complex molecules have been found in both theoretical [15] and experimental [16–20] studies of carbon nuclei.

To investigate the impact of extra neutrons on cluster structure in carbon isotopes, the first step is to examine the ^{13}C nucleus with one neutron added to the already well-studied ^{12}C nucleus. While most of the low-lying states can be described within the Shell Model, the states at higher excitation energies may start to exhibit more exotic structures, where an additional

neutron is expected to stabilize the 3α configurations found in ^{12}C. Different structures are proposed to appear, such as an analogue to the Hoyle state [21–23] and bent linear-chain structures [24, 25].

Of significant interest is the structure of the proton-rich ^{11}C nucleus. The ^{11}C nucleus and its isobaric analog ^{11}B can provide clues regarding the interplay between boson (α particle) and fermion degrees of freedom which develop into clustering in some instances. There is a strict similarity in the structure of these two nuclei with developed clustering [26–29] which can be connected with the 3α-cluster structure of ^{12}C. The signature of the three-center structure is the three-body decay of excited states which was observed for the ^{11}B states [30, 31] but its counterpart in ^{11}C has not been identified yet.

Experimental data on excited states of carbon isotopes are an important benchmark for theoretical models and additional studies are essential to improve understanding of the nature of three- and more-centers clustering.

2. Experimental setup

To study clustering in a broad range of light nuclei (concentrating mostly on carbon isotopes), the experiment was performed at the INFN-LNL in Legnaro, Italy, using the Tandem accelerator to accelerate a ^{14}N beam to 95 MeV. Beam was focused on several targets, all containing ^{10}B, but with different thicknesses and backings. The data presented here are collected using a 201 μm/cm^2 ^{10}B target with a thin formvar backing. The detector setup consisted of 6 detector telescopes each consisting of a thick (4×1000 μm and 2×500 μm) double-sided E and thin (6×20 μm) single-sided ΔE detector. Both detectors are divided into 16 strips, with the E detector having strips on each side forming an area of 256 pixels, and the ΔE detector only on one side. Due to this segmentation, the detection angle is precisely known. The detectors were set to cover polar angles ranging from 15° to 72°, while one-pixel coverage is up to a degree.

The lower end of the energy range was calibrated with a triple-alpha source (^{239}Pu, ^{241}Am, ^{244}Cm), while the higher end with elastic scattering of the ^{14}N beam on a thin gold target. Corrections due to energy loss in dead layers of a detector were included. To identify reaction products, the standard ΔE–E approach was used where energy deposited in the E detector is plotted *versus* energy loss in ΔE as shown in Fig. 1. Different isotopes, ranging from He to O are separated in clearly seen loci. The ΔE–E spectra were fitted semiautomatically using a multiparameter functional [32], from where, by application of 1-D cuts, different isotopes were selected.

Depending on different reaction exit channels and detector combinations, high or lower statistics data were collected and, therefore, different binning was used to present experimental data, ranging from 50 keV to 200 keV.

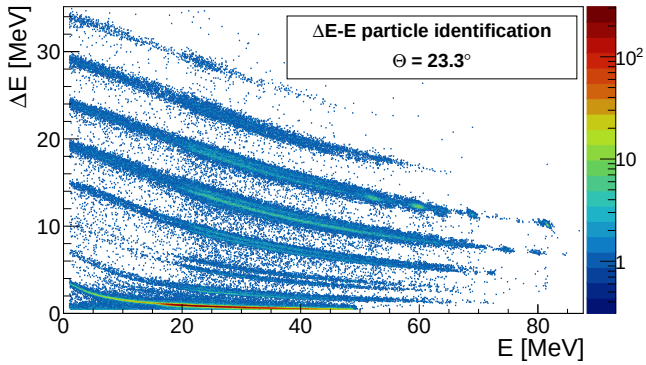

Fig. 1. Typical example of the particle identification spectrum obtained with the silicon strip detector telescopes for one pixel at the polar angle of 23.3°.

3. Analysis and results

Both single-hit and coincidence data were obtained during the experiment aiming to study reaction exit channels with two reaction products (at least one of them detected) and three reaction products (at least two of them detected). Analysis was conducted on all possible combinations of detected reaction products in different detector telescopes separately to minimize systematic errors from the ΔE detectors' nonuniformity, uncertainty of detector array geometry, and energy-loss calculations, as well as to minimize the effect of background contributions. If a peak was observed in more than one combination, it is considered to be a candidate for a state. Carbon nuclei of interest could be formed via the transfer of proton, deuteron, or triton from the beam to the target, and then decay into several exit channels

$$\begin{aligned} {}^{14}\mathrm{N} + {}^{10}\mathrm{B} &\rightarrow {}^{11}\mathrm{C}^{*} + {}^{13}\mathrm{C} \rightarrow {}^{7}\mathrm{Be} + {}^{4}\mathrm{He} + {}^{13}\mathrm{C} \\ &\rightarrow {}^{12}\mathrm{C}^{*} + {}^{12}\mathrm{C} \rightarrow {}^{8}\mathrm{Be} + {}^{4}\mathrm{He} + {}^{12}\mathrm{C} \\ &\rightarrow {}^{13}\mathrm{C}^{*} + {}^{11}\mathrm{C} \rightarrow {}^{9}\mathrm{Be} + {}^{4}\mathrm{He} + {}^{11}\mathrm{C}\,. \end{aligned} \tag{1}$$

The reactions with two products in the exit channel, with either both or a single one detected, were used to test and correct the estimated detector geometry by plotting spectra of excitation energy *versus* detected angles and checking the identification of the reaction channel. Using energy and momentum conservation laws, full kinematics of an event could be reconstructed and the excitation energy of the observed state can be determined. Even though single-hit data could give some insight into the cluster structure of carbon isotopes of interest, the focus of this report is on coincidence data for three-body reactions since direct detection of cluster decay of a nucleus is a strong indication of its cluster structure (see, for example, [8, 10, 12–14]).

An example of the analysis of such a three-particle reaction will be presented for the ^{10}B(^{14}N,^{12}C^{8}Be)^{4}He exit channel. It should be noted that ^{8}Be is unstable and decays into two ^{4}He particles. Its ground state is a resonant state of 5.6 eV width at 92 keV, and in the analysis, it was reconstructed from the energy and momentum of two detected ^{4}He. Events corresponding to the detection of ^{8}Be(gs) were subsequently analyzed as the three-body reaction events. Since two products are detected, to identify the third one and to determine missing energy in the exit channel, we use a correlation plot called the Catania plot [33]. Knowing the energy and momentum of two out of three products, using conservation laws one can easily determine the energy and momentum of the third product. Calculating and plotting new variables $\tilde{E} = E_3 - Q = E_p - E_1 - E_2$ and $\tilde{P} = p_3^2/2m_u$ for each event, we obtain event distribution which shows ridges differing by slope and y-axis intersection. To correctly identify the exit channel, we look at the slope of the line for the mass of the third undetected particle and at the y-axis intersection for the Q value of the reaction. Combining the Catania plot and projected Q-value spectra, one can make cuts to choose events corresponding to the exit channel of interest and to identify the origin of the selected data.

Figure 2 shows the Catania plot and Q-value spectrum for the mentioned reaction. Here, ^{4}He was undetected, while the other two products were detected, with the energy and momentum of ^{8}Be being reconstructed using conservation laws from two ^{4}He detected in the same detector. Slopes of the observed loci correspond to a value of A of an undetected particle equal to 4, confirming the identification of the reaction channel. Two distinct loci present in the plot differ by y-axis intersection where the lower one represents the reaction channel with all products in the ground state, and the higher one with ^{12}C in the first excited 4.44 MeV (2^+) state. Reaction products could result from decay of several intermediate states of ^{12}C, ^{16}O, and ^{20}Ne. To distinguish between these states, correlation plots between relative energies with added decay thresholds, *i.e.* excitation energies, of two of the

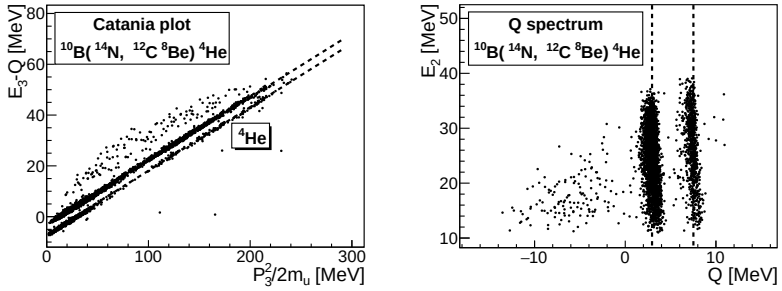

Fig. 2. Catania plot (left) and Q-value spectrum (right) for the ^{10}B(^{14}N, ^{12}C^{8}Be) ^{4}He reaction. Two loci represent events with all products in their ground state and with ^{12}C excited to the 4.44 MeV (2^+) state.

three possible intermediate products were examined (Fig. 3). Since we are interested in ^{12}C states, we discard ^{16}O intermediate states with a cut at around 17 MeV as shown in Fig. 3. The projection of this plot on its y-axis is the excitation spectrum of ^{12}C (Fig. 3). Observed peaks at 7.2 MeV, 9.3 MeV, and 13.7 MeV are indicated with dashed lines, and with a systematic shift of $\approx$ 400 keV, they move to 7.6 (0^+), 9.64 (3^-), and 14.1 (4^+) MeV which correspond to already well-known states. This shift originates from

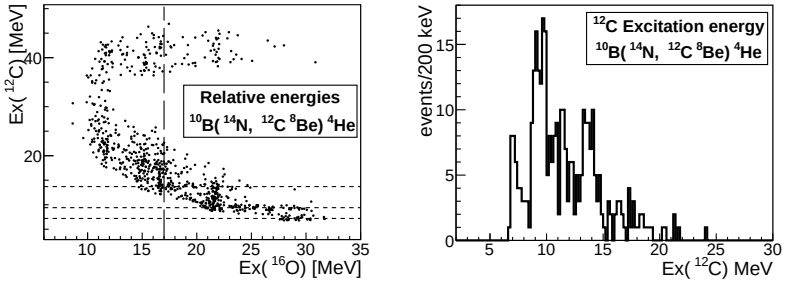

Fig. 3. Left: Correlation plot for the excitation energies of ^{12}C and ^{16}O with the vertical line representing separation at $\approx$ 17 MeV of ^{16}O intermediate states and horizontal lines representing the states in ^{12}C. Right: Excitation-energy spectrum for the decays of the ^{12}C excited states to $^{8}\mathrm{Be}_{\mathrm{gs}}$ and $^{4}\mathrm{He}_{\mathrm{gs}}$.

uncertainties in calculations of energy loss in the target and detectors' dead layers, as well as in the ΔE detector due to its large thickness nonuniformity, and uncertainties in the detectors' geometry. These affect the detectors' calibration and the reconstruction of the reaction event kinematics. In this case, the ^{12}C excitation energy is calculated from the energy and position of the detected recoil nucleus ^{12}C. The same systematic shift is expected in other presented excitation energy spectra as the ^{11,13}C excitation energies were calculated from the energy and position of the detected recoil ^{13,11}C.

One of the reaction exit channels to study ^{11}C is ^{10}B(^{14}N,^{13}C^{7}Be)^{4}He. With all reaction products in their ground state, detecting ^{13}C and ^{7}Be and proceeding with the same analysis procedure, relative energies spectrum and excitation spectrum shown in Fig. 4 are obtained. The dashed line indicates a peak at 8.2 MeV, which, due to the experimental resolution and shift, could correspond to a mixture of states at 8.4 MeV ($5/2^-$) and a doublet around 8.7 MeV ($7/2^+$ and $5/2^+$).

Furthermore, the decay of ^{13}C to ^{9}Be and ^{4}He was examined using the ^{10}B(^{14}N,^{11}C^{9}Be)^{4}He data. The 2-D correlation plot and excitation-energy spectrum with ^{11}C and ^{9}Be detected in their ground states are shown in Fig. 5. The broad peak centered at $13.6 + 0.4 = 14$ MeV clearly stands out and is marked with the dashed line. To this peak may contribute previously observed states at excitation energies from 13 to 15.5 MeV.

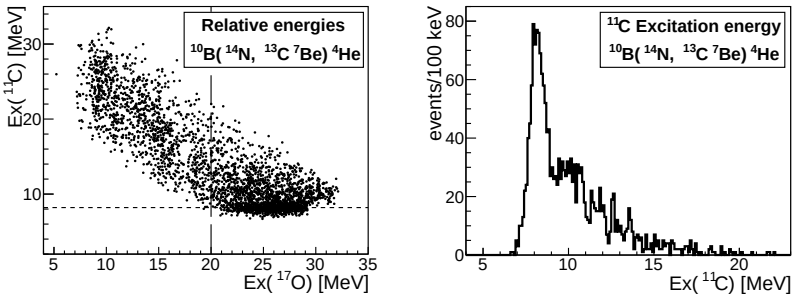

Fig. 4. Left: Correlation plot for the excitation energies of ^{11}C and ^{17}O with the vertical line representing separation at $\approx$ 20 MeV of ^{17}O intermediate states and the horizontal line representing the state in ^{11}C. Right: Excitation-energy spectrum for the decays of the ^{11}C excited states to $^{7}\mathrm{Be}_{\mathrm{gs}}$ and $^{4}\mathrm{He}_{\mathrm{gs}}$.

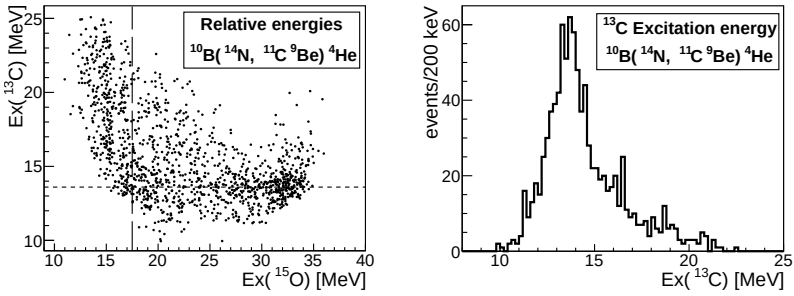

Fig. 5. Left: Correlation plot for the excitation energies of ^{13}C and ^{15}O with the vertical line representing separation at $\approx$ 17.5 MeV of ^{15}O intermediate states and the horizontal line representing the state in ^{13}C. Right: Excitation-energy spectrum for the decays of the ^{13}C excited states to $^{9}\mathrm{Be}_{\mathrm{gs}}$ and $^{4}\mathrm{He}_{\mathrm{gs}}$.

4. Conclusion

In this report, are presented the preliminary results of the measurement of the ^{10}B(^{14}N,^{X}C^{Y}Be) ^{4}He (X = 13,12,11; Y = 7,8,9) reactions. The observed ^{Y}Be+^{4}He decays of the ^{11,12,13}C excited states are in good agreement with published results. The observation of these states serves as an important test of the analysis and data selection procedure and it is the first step in the study of clustering in C isotopes. Discussion of the structure of the observed states, analysis of other exit channels such as ^{10}B(^{14}N,^{11}C^{8}Be)^{5}He, ^{10}B(^{14}N,^{13}C^{8}Be)^{3}He, ^{10}B(^{14}N,^{13}C^{10}B)^{1}H, and a detailed study of the cluster structures of ^{11,12,13}C excited states will be given in the forthcoming publications.

This work has been supported in part by the Croatian Science Foundation under Project No. IP-2018-01-1257, and in part by the Center of Excellence for Advanced Materials and Sensing Devices (grant No. KK.01.1.1.01.0001).

REFERENCES

[1] M. Freer *et al.*, *Rev. Mod. Phys.* **90**, 035004 (2018).
[2] W. von Oertzen, M. Freer, Y. Kanada-En'yo, *Phys. Rep.* **432**, 43 (2006).
[3] M. Freer, *Rep. Prog. Phys.* **70**, 2149 (2007).
[4] W.R. Zimmerman *et al.*, *Phys. Rev. Lett.* **110**, 152502 (2013).
[5] M. Freer *et al.*, *Phys. Rev. C* **80**, 041303 (2009).
[6] M. Freer *et al.*, *Phys. Rev. C* **86**, 034320 (2012).
[7] M. Freer *et al.*, *Phys. Rev. C* **83**, 034314 (2011).
[8] D. Jelavić Malenica *et al.*, *Phys. Rev. C* **99**, 064318 (2019).
[9] D.J. Marín-Lámbarri *et al.*, *Phys. Rev. Lett.* **113**, 012502 (2014).
[10] C. Wheldon *et al.*, *Phys. Rev. C* **90**, 014319 (2014).
[11] M. Freer *et al.*, *Phys. Rev. Lett.* **96**, 042501 (2006).
[12] M. Milin *et al.*, *Nucl. Phys. A* **753**, 263 (2005).
[13] N. Soić *et al.*, *Europhys. Lett.* **34**, 7 (1996).
[14] N. Vukman *et al.*, *Front. Phys.* **10**, 1009421 (2022), and references therein.
[15] N. Itagaki *et al.*, *Phys. Rev. C* **64**, 014301 (2001).
[16] N. Soić *et al.*, *Nucl. Phys. A* **728**, 12 (2003).
[17] D.L. Price *et al.*, *Nucl. Phys. A* **765**, 263 (2006).
[18] M. Freer *et al.*, *Phys. Rev. C* **84**, 034317 (2011).
[19] C. Wheldon *et al.*, *Phys. Rev. C* **86**, 044328 (2012).
[20] D. Jelavić Malenica *et al.*, *Eur. Phys. J. A* **59**, 228 (2023).
[21] T. Yamada, Y. Funaki, *Phys. Rev. C* **92**, 034326 (2015).
[22] T. Yamada, Y. Funaki, *Int. J. Mod. Phys. E* **20**, 910 (2011).
[23] T. Kawabata *et al.*, *Int. J. Mod. Phys. E* **17**, 2071 (2008).
[24] N. Furutachi, M. Kimura, *Phys. Rev. C* **83**, 021303 (2011).
[25] N. Itagaki, W. von Oertzen, S. Okabe, *Phys. Rev. C* **74**, 067304 (2006).
[26] N. Soić *et al.*, *Nucl. Phys. A* **742**, 271 (2004).
[27] Y. Kanada-En'yo, *Phys. Rev. C* **75**, 024302 (2007).
[28] M. Freer *et al.*, *Phys. Rev. C* **85**, 014304 (2012).
[29] H. Yamaguchi *et al.*, *Phys. Rev. C* **87**, 034303 (2013).
[30] N. Soić *et al.*, *J. Phys. G: Nucl. Part. Phys.* **31**, S1701 (2005).
[31] N. Curtis *et al.*, *Phys. Rev. C* **72**, 044320 (2005).
[32] L. Tassan-Got, *Nucl. Instrum. Methods Phys. Res. B* **194**, 503 (2002).
[33] E. Costanzo *et al.*, *Nucl. Instrum. Methods Phys. Res. A* **295**, 373 (1990).